MATERIALS PHYSICS AND MECHANICS RESEARCH ARTICLE

Submitted: July 11, 2024 **Revised: March 20, 2025** **Accepted: May 31, 2025**

Enhancing EDM performance of Monel-400 super alloy through process parameter optimization: RSM-based experimental and microstructural analysis

M.R. Panda [1], S.K. Mishra [2] ✉, P.K. Sahoo [1]

[1] GIET University Gunupur, Rayagada, India

[2] VSSUT Burla, Odisha, India

✉ srimantnitrkl@gmail.com

ABSTRACT

A nickel-copper alloy Monel-400 renowned for its corrosion resistance and thermal properties finds extensive application in chemical, fitting, fastener, and marine industries. However, machining intricate, delicate components from this alloy using conventional methods presents significant challenges. EDM is a non-traditional process capable of producing precise, high-quality surfaces, which emerges as a viable alternative. The die-sinking EDM of Monel-400 are investigated with a particular focus on the machined surface microstructure. A Box-Behnken design was employed to evaluate the influence of discharge current, pulse-on time, and voltage gap on material removal rate, tool wear rate, and surface roughness. Results indicate that impact of peak current and pulse-on time are primary determinants of Monel-400 machining characteristics. While impact of peak current exhibited the most significant impact on MRR, pulse-on time was identified as the critical factor affecting tool wear rate and surface roughness. A comprehensive metallographic examination of the machined surface was conducted to elucidate wear mechanisms.

KEYWORDS

EDM • Monel-400 alloy • microstructure • RSM • box-behnken design • SEM

Acknowledgements. *The author M.R. Panda and P. K. Sahoo would like to express their sincere gratitude to all those who contributed to the successful completion of this research. Special thanks to the Department of Mechanical Engineering at GIET University Gunupur, Odisha, for providing the necessary resources and facilities.*

Citation: Panda MR, Mishra SK, Sahoo PK. Enhancing EDM performance of Monel-400 super alloy through process parameter optimization: RSM-based experimental and microstructural analysis. *Materials Physics and Mechanics*. 2025;53(3): 24–36.
http://dx.doi.org/10.18149/MPM.5332025_3

Introduction

Electrical discharge machining (EDM) is a computer-controlled, non-traditional machining process that utilizes a series of controlled electrical discharges (sparks) to remove material from the workpiece. The electric spark produced as a result of potential difference is mainly used as the cutting tool to cut (erode) the material [1]. EDM is mainly applied to the family of materials that are difficult to machine by traditional manufacturing techniques, but the process is limited to conductive materials only [2]. Due to its beneficial properties like better strength-to-weight ratio and corrosion resistance, super alloys such as Monel-400 find widespread uses in aircraft, oil production and refining, musical instruments, valves, fasteners and maritime applications [3]. Monel-400 alloy's poor thermal diffusivity causes high tool tip temperatures during traditional machining, rendering traditional methods inefficient [4,5]. Non-traditional techniques, such as EDM, offer a more viable approach to

machining this challenging material. Several process parameters, including electrode material, discharge current, pulse-on time, duty cycle, and gap voltage, significantly influence EDM performance when machining Monel-400 alloy [6]. Copper, brass and graphite are mainly used as electrode materials due to their high melting point and conductivity [7]. Owing to its better load bearing and non-corrosive properties, Monel-400 is hardened by the cold working process as a result it becomes very tough to machine by conventional machining [8,9]. Monel-400 has an electrical conductivity of roughly 34 % IACS, a specific gravity of 8.80, a melting point temperature of 1300–1350 °C, and a hardness of 65 Rockwell. Monel-400 offers exceptional toughness that is maintained across a wide temperature range [10–14].

Optimizing process parameters is critical to enhancing the efficiency of EDM when applied to the Monel-400 superalloy. Because of its inherent high strength and poor heat conductivity, Monel-400 presents significant challenges to traditional machining methods, necessitating the exploration of alternative processes like EDM [15,16]. Research suggests that advanced techniques like Wire EDM and Electrical Discharge Diamond face grinding (EDDFG) show promise in improving material removal rates and surface quality for Monel-400 components [15,17]. By meticulously controlling process parameters such as pulse duration and applied current, and by judiciously selecting electrode materials, substantial enhancements in machining efficiency and precision can be realized [16,18]. The use of modern optimization techniques like as Taguchi analysis and genetic algorithms has the potential to improve Monel-400's EDM process, leading in higher performance and lower costs [17–19]. Gupta and Gupta [20], Shanmugha Sundaram [21], and Amuthak Kannan et al. [22] investigated the EDM of hybrid Al-Al_2O_3/B_4C, Al-Si alloy-graphite, and basalt fiber composites, respectively. Their research focused on identifying optimal process parameter combinations for these materials. Gopala Kannan et al. [8] investigated the EDM of a novel aluminum 7075 matrix composite reinforced with 10 % Al_2O_3 particles using a copper electrode. The impact of process factors on MRR, TWR, and SR was investigated using a mathematical model based on response surface methodology (RSM). Furthermore, ANOVA was used to determine the impact of peak current (I_p), pulse-on time (T_{on}), voltage (V), and pulse-off time (T_{off}) on EDM performance. Jahan et al. [10] investigated the optimization of surface finish during the EDM of WC composites, renowned for their exceptional hardness, strength, and wear resistance. Their study explored the influence of electrode materials, including tungsten, copper tungsten, and silver tungsten. Sivasankar et al. [23] studied EDM performance on ZrB_2 using a wide range of electrode materials such as graphite, aluminum, tantalum, niobium, copper, brass, silver, tungsten, and titanium. Their research focused on hole quality metrics, including roundness, form, and diameter are among the usual EDM responses, along with SR, MRR, and TWR. A desirability function analysis was carried out to assess tool performance. Assarzadeh and Ghoreishi [24] proposed a dual response surface-desirability method for modeling and optimizing process parameters in Al_2O_3 powder-mixed electrical discharge machining (PMEDM).

After a far-reaching and comprehensive investigation of the published works of literature, numerous gaps were figured out in the EDM process. The majority of experimenters or analysts have probed the effect of the finite number of machining parameters in the computation of results or execution on the machined surface on EDM.

Also observed inadequate exploration of the microstructural changes and their influence on EDM performance. The purpose of this study was to investigate the effects of pulse-on time, peak current, and voltage gap on Monel-400 electrical discharge machining (EDM). Response surface methodology (RSM) was used to optimize these process parameters in order to maximize material removal rate (MRR) while decreasing surface roughness (*Ra*) and tool wear rate (TWR). To further understand the material's behavior to different process parameter combinations, a complete microstructural examination of the machined surfaces was performed, including the recast layer, heat-affected zone, and worn tool surfaces.

Materials and Methods

The Monel-400 alloy used as the workpiece material in this study is a commercially available nickel–copper alloy, procured from M/s Metal Mart Pvt. Ltd., Mumbai, India. The alloy is composed primarily of nickel (~ 63 %) and copper (~ 30 %), with minor quantities of iron, manganese, silicon, and carbon. The typical chemical composition of Monel-400 is reported in Table 1.

Table 1. Chemical composition of selected material

Element	Ni	Cu	Fe	Mn	Si	C
Wt. %	63.0	30.0	2.5	2.0	0.5	0.3

The alloy sheet was supplied in a cold-rolled condition with a thickness of 5 mm and was subsequently cut into rectangular samples of 50 × 50 mm² using a precision abrasive cutter to maintain dimensional accuracy and edge integrity. The copper electrode, with a diameter of 9 mm, was sourced from M/s ElectroTech Supplies, Bhubaneswar, India. The electrode material was electrolytic copper with a purity of 99.9 %, chosen for its high electrical and thermal conductivity.

Investigations are performed in the die-sinking NC EDM machine shown in Fig. 1 by maintaining a constant servo head gap. The EDM 30 dielectric oil was supplied by Hindustan Petroleum Corporation Ltd., having a specific gravity of 0.8 at room temperature. It was used without any additives to ensure consistency across all trials.

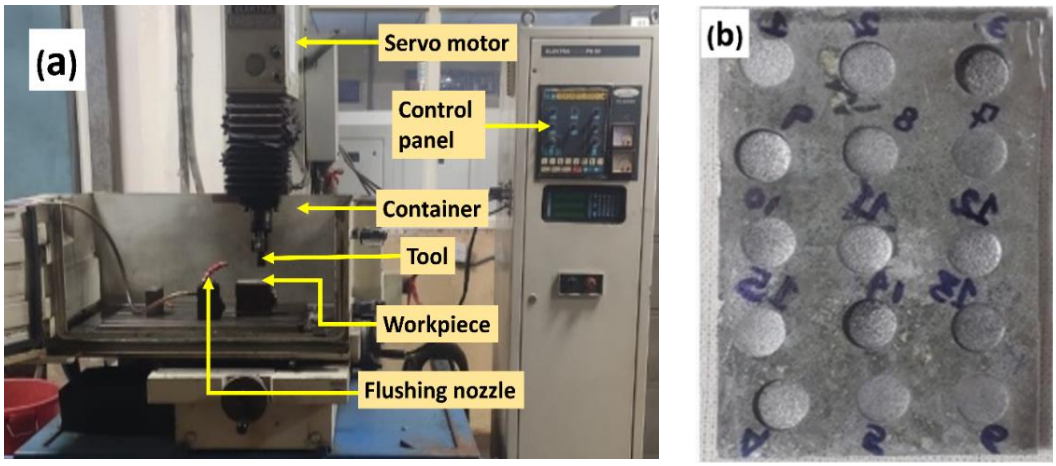

Fig. 1. Illustration of EDM machining: (a) EDM machine, (b) workpiece material after machining

Because electrical conductivity is a critical need for EDM electrodes, copper was chosen as the electrode material for this experiment. All materials were inspected for quality prior to experimentation. The Monel-400 workpieces were cleaned with acetone to remove surface contaminants, while the copper electrodes were polished to ensure proper electrical contact during the machining process. Each experimental run consists of 3 min of machining time. A precision electronic weight-measuring machine is used after each experimental run to determine the material loss from the tool and workpiece.

In EDM of Monel-400, careful selection of process parameters is essential due to the alloy's high strength and low thermal conductivity, which can complicate machining. Parameters such as pulse current, pulse on-time, and pulse off-time were chosen based on their known influence on key performance indicators like material removal rate (MRR), tool wear rate (TWR), and surface roughness. These parameters directly affect spark energy, discharge frequency, and cooling time between sparks, making them critical for efficient and stable machining. The range for each parameter was established through a combination of literature review and preliminary experiments to ensure a comprehensive yet practical design space. Table 2 shows the values of chosen process parameters. The order of parameters is selected in such a way that the experimentation on the workpiece can be conducted smoothly to achieve accomplishment. The rest parameters are polarity, flushing pressure, and duty cycle held constant throughout the experiment.

Table 2. Process parameters and their order

Process parameter	**Symbol**	**Unit**	**Order**		
			Order -1	**Order 0**	**Order 1**
Pulse on time	(T_{on})	µs	500	1000	2000
Peak current	(I_p)	A	18	33	50
Voltage	(V)	V	3	7	10

Table 3. Experimental layout

		Factor 1	Factor 2	Factor 3	Response 1	Response 2	Response 3
Std	**Run**	**A: Peak current**	**B: Pulse on time**	**C: Voltage gap**	**MRR, mm^3/min**	**TWR, mm^3/min**	**Surface roughness, µm**
8	1	1	0	1	26.515	1.737	2.031
2	2	1	-1	0	20.83	1.86	2.382
4	3	1	1	0	66.28	3.78	3.955
11	4	0	-1	1	3.78	0.567	1.226
9	5	0	-1	-1	18.93	0.894	1.392
7	6	-1	0	1	5.68	0.782	1.3
3	7	-1	1	0	9.56	2.87	2.987
10	8	0	1	-1	5.68	3.24	3.453
6	9	1	0	-1	32.19	2.65	2.518
1	10	-1	-1	0	11.26	0.456	1.15
13	11	0	0	0	7.575	1.864	2.455
14	12	0	0	0	7.575	1.864	2.223
12	13	0	1	1	22.72	3.065	3.151
15	14	0	0	0	7.12	1.864	2.223
5	15	-1	0	-1	6.54	1.2	1.625

Design of experiment

The design of experiment is arranged in accordance with the RSM Box-Behnken design. Fifteen investigations are performed on the workpiece. Subsequently, as per the experimental design obtained from Design Experts software, the machining on Monel-400 is executed. During the machining, the dielectric fluid was continuously flushing on the machining surface to clean the surface from debris. Table 3 depicts the different experiment arrangements.

Measurement of responses

Material removal rate (MRR) may be defined as the rate of material removed from the surface of the workpiece per unit time. The equation used for the evaluation of MRR is mentioned below [25]: $\mathbf{MRR}\left(\frac{\mathbf{mm^3}}{\mathbf{min}}\right) = \frac{\boldsymbol{Mw1-Mw2}}{\boldsymbol{t\times\rho}}$, where machining time t = 3 min (fixed), a density of MONEL-400 material is ρ = 8800 kg/m^2, $\boldsymbol{Mw1}$ is a mass of workpiece material prior to machining, $\boldsymbol{Mw2}$ is a mass of workpiece material after machining.

Tool wear rate (TWR) may be defined as the rate of material removed from the surface of the tool material per unit time. The TWR is calculated by using the following equation [26]: $\mathrm{TWR}\left(\frac{\mathrm{mm^3}}{\mathrm{min}}\right) = \frac{Mt1-Mt2}{t\times\rho}$, where t is machining time, density of copper is ρ = 8940 kg/m^2, Mt_1 is a mass of tool material prior to machining, Mt_2 is a mass of the tool material after machining.

A surface roughness (SR) analyser (model SJ-410, portable type) was used to quantify R. The instrument's parameters were set at 4 Pa measurement force, 25 mm evaluation length, and 0.000125 μm resolution.

Performance evaluation

To explore the influence of process variables on response parameters, a Box-Behnken design was used in conjunction with response surface methodology (RSM). This experimental design necessitated a minimum of fifteen experimental runs, including three center points. ANOVA was used to determine the contribution of each input parameter to the output responses. Table 3 shows how different machining factors affect the reaction.

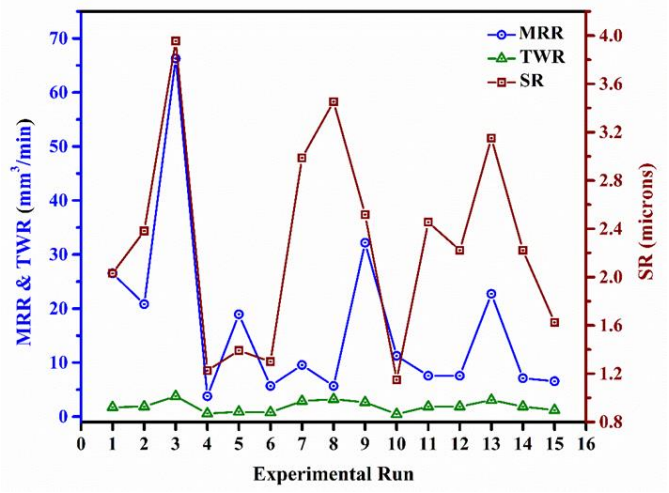

Fig. 2. MRR, TWR and SR plot for each experimental run

Figure 2 shows the plot for responses for each experimental run. As evident from the graphical representation, the optimum value for all three measured responses were obtained during the third experimental run, conducted with pulse on time of 2000 µs, current of 50 A, and voltage of 7 V. Furthermore, the plot clearly indicates a positive correlation between increasing current and pulse on time and the resulting material removal rate from both the workpiece and the tool surface. This enhanced material removal consequently leads to an increase in surface roughness.

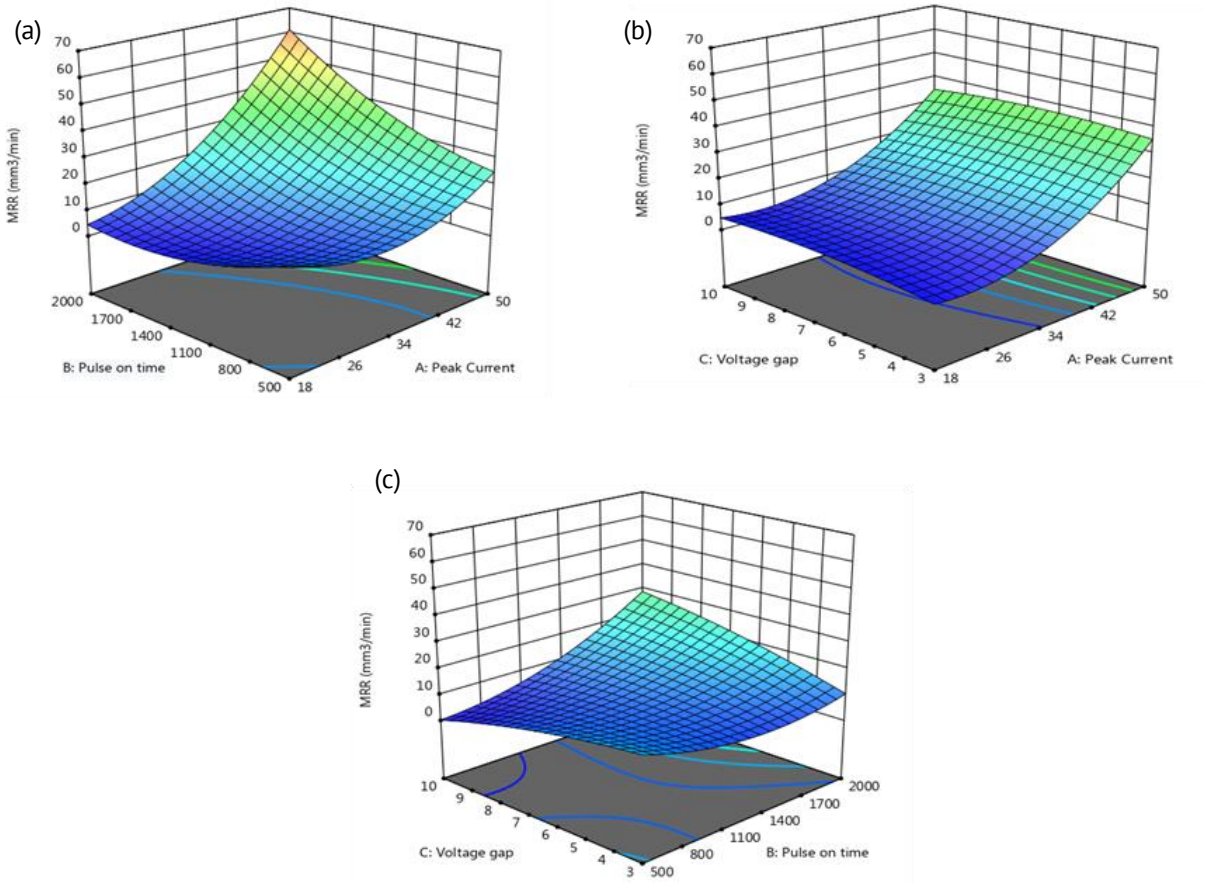

Fig. 3. Surface plot of MRR with (a) T_{on} and I_p, (b) voltage and I_p, (c) T_{on} and voltage gap

Table 4 presents the ANOVA table for rate of material removal, excluding non-significant variables. T_{on} (B), I_p (A), the quadratic term A^2, and interaction terms AB and AC were determined to be highly significant. *Ip* demonstrated the most significant impact on MRR, accounting for 53.34 % of the response. The surface plots in Fig. 3 illustrate the relationship between MRR, pulse-on time (T_{on}), peak current (I_p), and voltage gap (V). Figure 3(a,b) demonstrates a positive correlation between MRR and both T_{on} and I_p. This is due to the direct relationship between current and spark density, which causes more material removal at higher current levels. Similarly, with an increase in T_{on}, the discharging of the spark occurs for a longer duration hence resulting in greater material removal. Extended pulse-on time (T_{on}) facilitates deeper heat flux penetration into the workpiece, promoting the formation of a larger plasma area and consequently enhancing material removal rate (MRR) significantly [27,28]. As depicted in Fig. 3(b,c), a marginal increase in MRR is observed with escalating voltage.

Table 4. ANOVA for response 1: for MRR

Source	Sum of squares	DF	Mean square	F-value	p-value		% contribution
Model	3585.68	9	398.41	16.77	0.0032	significant	
A-peak current	1975.87	1	1975.87	83.19	0.0003		53.34
B-pulse on time	280.68	1	280.68	11.82	0.0185		7.57
C-voltage gap	4.79	1	4.79	0.2015	0.6723		0.13
AB	629	1	629	26.5	0.0036		17.0
AC	4.94	1	4.94	0.208	0.6675		0.133
BC	304.8	1	304.8	12.83	0.0158		8.22
A^2	460	1	460	19.4	0.0070		12.41
B^2	96.7	1	96.7	4.07	0.0996		2.61
C^2	13.27	1	13.27	0.5585	0.4885		0.36
Residual	118.76	5	23.75				3.20
Lack of fit	118.62	3	39.54	573.0	0.0017	not significant	3.20
Pure error	0.140	2	0.07				0.00372
Cor total	3704.43	14					

Table 5. ANOVA for response 2: for TWR

Source	Sum of squares	DF	Mean quare	F-value	p-value		% contribution
Model	14.71	9	1.63	68.44	0.0001	significant	
A-peak current	2.78	1	2.78	116.52	0.0001		18.74
B-pulse on time	10.53	1	10.53	440.74	< 0.0001		71
C-voltage gap	0.4200	1	0.4200	17.58	0.0085		2.83
AB	0.0610	1	0.0610	2.55	0.1709		0.41
AC	0.0613	1	0.0613	2.56	0.1702		0.41
BC	0.0058	1	0.0058	0.2418	0.6438		0.039
A^2	0.0007	1	0.0007	0.0308	0.8675		0.004
B^2	0.4875	1	0.4875	20.41	0.0063		3.28
C^2	0.3018	1	0.3018	12.63	0.0163		2.035
Residual	0.1195	5	0.0239				0.805
Lack of fit	0.1195	3	0.0398			not significant	0.805
Pure error	0.0000	2	0.0000				0.0000
Cor total	14.83	14					

Table 5 shows the ANOVA table for TWR subsequent rejection of all unimportant variables. The Model F-value of 68.44 implies the model is significant. With a 71 % contribution, pulse on time proves to be the most influencing factor for TWR followed by peak current. In this case, A, B, C, B^2, and C^2 are significant model terms.

Figure 4 indicates the surface plots for TWR against pulse on time (T_{on}), peak current (I_p), and voltage gap (V). It clearly shows that, with an increase in current that to for a longer duration of time, a large amount of heat accumulates at the tool surface which subsequently results in higher tool wear. With an increase in current and time of

discharging the TWR increases while the increase in voltage gap results in a decrease of wear rate on the tool.

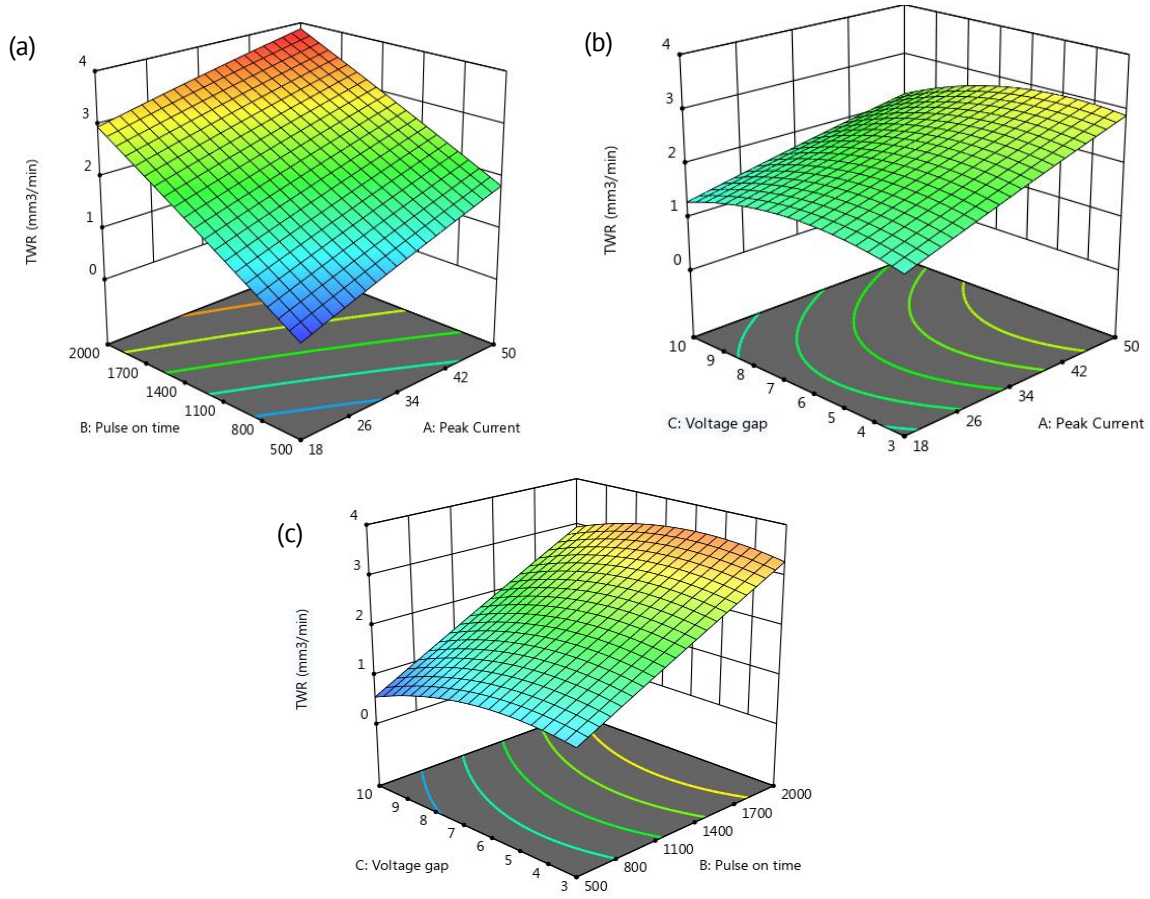

Fig. 4. Surface plot of TWR with (a) pulse on time and peak current, (b) voltage and peak current, (c) pulse on time and voltage gap

Table 6. ANOVA for response 3: for SR

Source	Sum of squares	DF	Mean square	F-value	P-value		% contribution
Model	10.04	9	1.12	41.73	0.0004	significant	
A-peak current	1.83	1	1.83	68.40	0.0004		17.994
B-pulse on time	6.84	1	6.84	255.86	< 0.0001		67.25
C-voltage gap	0.2048	1	0.2048	7.66	0.0394		2.01
AB	0.0174	1	0.0174	0.6520	0.4561		0.17
AC	0.0066	1	0.0066	0.2455	0.6413		0.06
BC	0.0046	1	0.0046	0.1730	0.6947		0.04
A^2	0.0130	1	0.0130	0.4878	0.5161		0.12
B^2	0.5264	1	0.5264	19.70	0.0068		5.17
C^2	0.5121	1	0.5121	19.16	0.0072		0.0503
Residual	0.1336	5	0.0267				1.31
Lack of fit	0.0977	3	0.0326	1.82	0.3744	not significant	0.953
Pure error	0.0359	2	0.0179				0.3529
Cor total	10.17	14					

Table 6 shows the ANOVA table. The model shows that pulse on time has the highest contribution (67 %) in the formation of SR. In this case, A, B, C, B^2, and C^2 are significant model terms. In the EDM process, the surface mainly produced dues presence of different surface irregularities such as craters, cracks, globules and debris, etc. It is evident from the surface plot (Fig. 5) of surface roughness with I_p and T_{on} that, both the parameters are directly proportional to SR. With an increase in current (I_p) the intensity of the spark increases and when this highly intense spark strikes the work surface, it results in the formation of large craters. Similarly, with an increase in T_{on}, the spark strikes the surface for a longer duration and with improper flushing the debris may accumulate over the machined surface resulting in an increase the roughness.

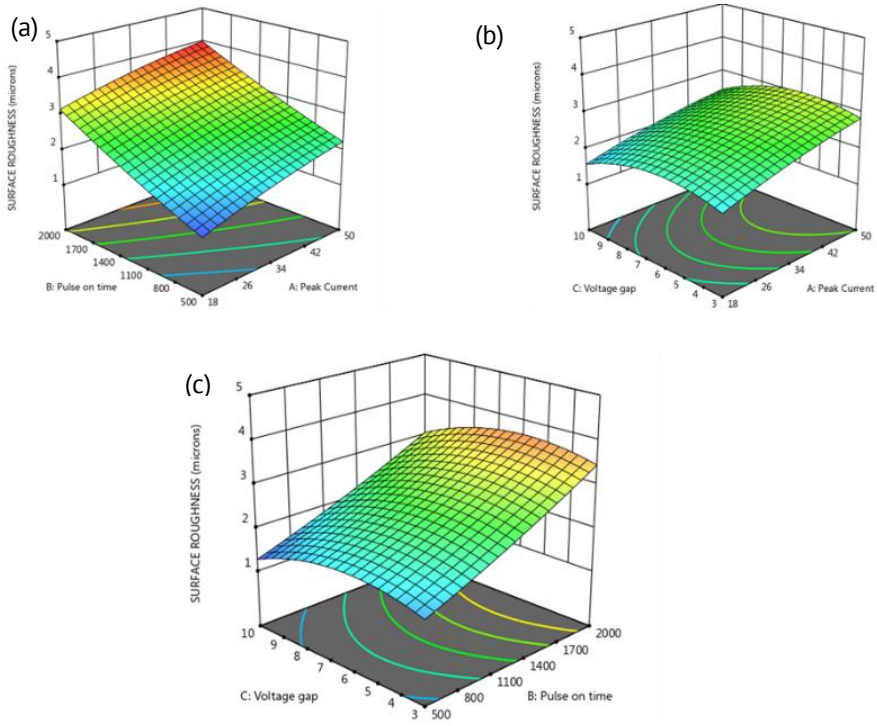

Fig. 5. Surface plot of *R*a with (a) pulse on time and peak current, (b) voltage and peak current, (c) voltage and pulse on time

The coefficient of determination (R^2) and adjusted R^2 of the developed model were found to be more than 95 % for all the responses, hence it is concluded that the lack of fit is not significant for all the responses.

Microstructural analysis

A microstructural analysis is carried out to the extent of evaluation of microstructure at the machined surface on the workpiece at different magnification levels. The microstructure of a material can strongly influences physical properties such as strength, toughness, ductility, hardness, corrosion resistance, etc. For this experiment, the Monel-400 superalloy has been taken for microstructural analysis after machining on EDM. The machined surfaces have been examined by SEM (scanning electron microscopy).

The spark in EDM is produced due to the movement of electrons and ions at very high kinetic energy between the two polarities in the dielectric medium. When these electrons and ions strike the surface of a workpiece or tool, it results in the conversion of kinetic energy into thermal energy or heat flux [29,30]. This intense localized heat flux at a high concentration of electrons and ions forms the plasma. Now upon withdrawal of the potential difference, the plasma channel bursts resulting in the formation of cracks and craters as shown in Fig. 6. Part of the molten material from the machined surface comes out as microchips may accumulate on the machined surface itself due to improper flushing is termed as debris or globules as depicted in Fig. 7(a).

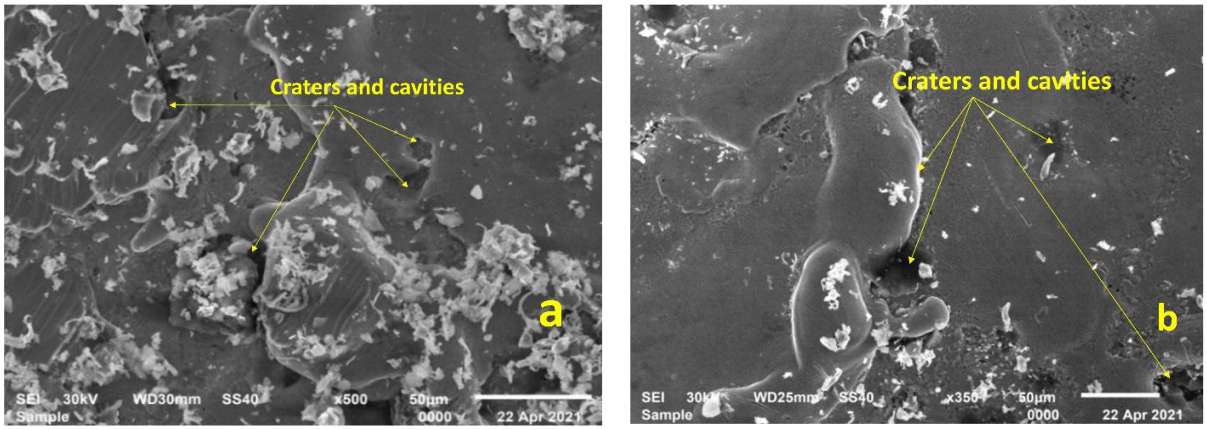

Fig. 6. Depiction of craters and cavities (a) 500x SEM image for *Ip* = 33, T_{on} = 2000 and *V* = 10, (b) 350x SEM image for I_p = 50, T_{on} = 1000, *V* = 7

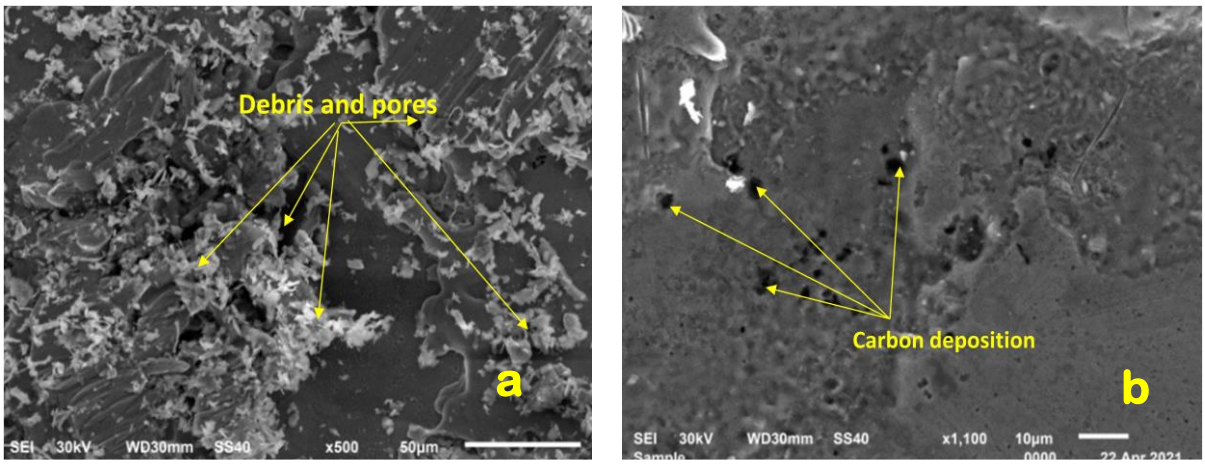

Fig. 7. (a) Formation of Debris, pores at the machined surface for I_p = 50, T_{on} = 1000, *V* = 3 and (b) carbon deposition at 1100x for I_p = 50, T_{on} = 2000, *V* = 7

Figure 7(b) shows the carbon particles getting deposited on the machined surface; this may be due to the burning of dielectric molecules in the plasma channel. At the time of the EDM machining process, a tremendous amount of heat is produced which melts the metal's surface. After machining, the metal experiences ultra-rapid cooling termed "quenching" due to flushing by dielectric fluid. A layer formation occurs on the workpiece surface explicated as a recast layer after solidification, as shown in Fig. 8. From micrographs, the thickness of the recast layer was calculated and found to be 81 μm.

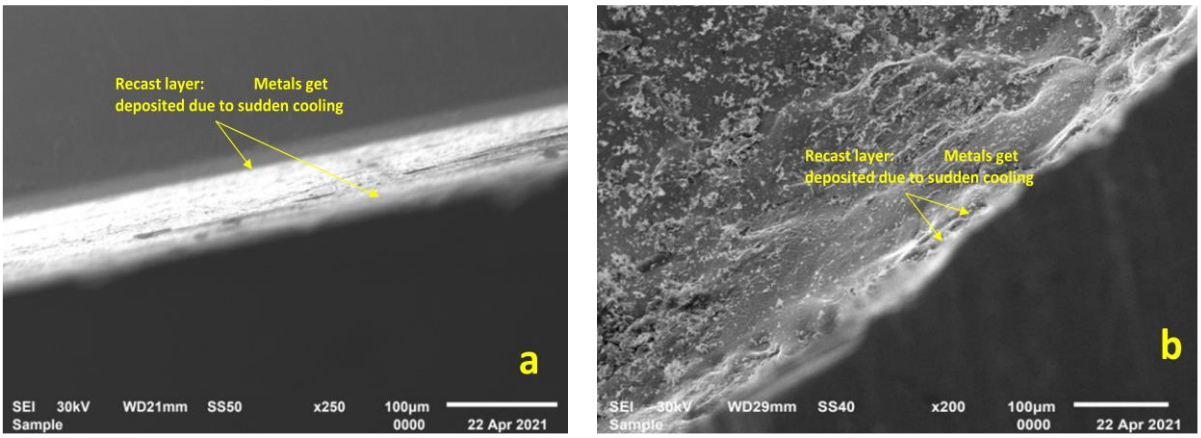

Fig. 8. Depiction of Recast layer at the edge of the machined surface
(a) 250x SEM image for I_p = 50, T_{on} = 2000, V = 7, (b) 200x SEM image for I_p = 18, T_{on} = 500, V = 7

Conclusions

The empirical study on the impact of various EDM parameters on Monel-400 superalloy using cylindrical copper electrodes focused on key performance metrics such as material removal rate (MRR), tool wear rate (TWR), and surface roughness (SR). Subsequently, the correlation between process parameters and performance outputs was assessed utilizing response surface methodology (RSM), yielding the following conclusions:

1. From the findings of the result for MRR, peak current (I_p) played the most significant influencing factor with a 53.3 % contribution followed by pulse-on-time (T_{on}). Consequently, elevated I_p and T_{on} levels are correlated with enhanced MRR.
2. From the findings of the result for tool wear rate, the T_{on} played the most important influencing factor with a 71 % contribution followed by I_p. An increase in T_{on} and I_p correlates with an elevated tool wear rate, whereas an increment in inter-electrode-gap results in a marginal reduction of tool wear rate.
3. Analysis of surface roughness (SR) revealed that pulse-on-time (T_{on}) exerted the most significant influence, contributing 67 % to the response, followed by peak current (I_p). A better-machined surface can be obtained by limiting the values of Ton and Ip. It was also mentioned in some works of literature that, with effecting flushing the SR can be reduced.
4. Inter-electrode gap (IEG) was determined to have a negligible impact on all evaluated performance metrics.
5. Microstructure images revealed that most of the surface irregularities on the machined surface are obtained at higher levels of Ip and Ton. It can be reduced by proper flushing at the tool-workpiece interface.

CRediT authorship contribution statement

Manas R. Panda: writing – review & editing, writing – original draft, conceptualization, supervision; **Srimant K. Mishra**: writing – review & editing, supervision, data curation, **Prabin K. Sahoo**: writing – original draft, Investigation.

Conflict of interest

The authors declare that they have no conflict of interest.

References

1. Vikas, Shashikant, Roy AK, Kumar K. Effect and Optimization of Machine Process Parameters on MRR for EN19 & EN41 materials using Taguchi. *Procedia Technology.* 2014;14: 204–210.
2. Muthuramalingam T, Mohan B. A review on influence of electrical process parameters in EDM process. *Archives of Civil and Mechanical Engineering.* 2015;15(1): 87–94.
3. Kumar V, Kumar V, Jangra KK. An experimental analysis and optimization of machining rate and surface characteristics in WEDM of Monel-400 using RSM and desirability approach. *Journal of Industrial Engineering International.* 2015;11: 297–307.
4. Kuppan P, Rajadurai A, Narayanan S. Influence of EDM process parameters in deep hole drilling of Inconel 718. *The International Journal of Advanced Manufacturing Technology.* 2008;38(1–2): 74–84.
5. Kanagarajan D, Karthikeyan R, Palanikumar K, Paulo Davim J. Optimization of electrical discharge machining characteristics of WC/Co composites using non-dominated sorting genetic algorithm (NSGA-II). *The International Journal of Advanced Manufacturing Technology.* 2008;36(11–12): 1124–1132.
6. Kumar SS, Kumar N. Optimizing the EDM Parameters to Improve the Surface Roughness of Titanium Alloy (Ti-6AL-4V). *International Journal of Emerging Science and Engineering.* 2013;1: 2319–6378.
7. Mahalingam M, Varahamoorthi R. Investigation on tool wear rate of brass tool during machining of Monel-400 alloy using electric discharge machine. *Materials Today Proceedings.* 2020;26: 1213–1220.
8. Gopalakannan S, Thiyagarajan S, Kalaichelvan K. Modelling and Optimization of EDM of Al 7075/10wt% Al2O3 Metal Matrix Composites by Response Surface Method. Advanced Materials Research. *Advanced Materials Research.* 2012;488–489: 856–860.
9. Kung K, Chiang K. Modelling and analysis of machinability evaluation in the wire electrical discharge machining (wedm) process of aluminium oxide-based ceramic. *Materials and Manufacturing Processes.* 2008;23(3): 241–250.
10. Jahan MP, Wong YS, Rahman M. A study on the fine-finish die-sinking micro-EDM of tungsten carbide using different electrode materials. *Journal of Materials Processing Technology.* 2009;209(8): 3956–3967.
11. Lee SH, Li XP. Study of the effect of machining parameters on the machining characteristics in electrical discharge machining of tungsten carbide. *Journal of Materials Processing Technology.* 2001;115(3): 344–358.
12. Mahalingam M, Umesh BA, Varahamoorthi R. Effect of Wire Electric Discharge Machining Process Parameters on Surface Roughness of Monel 400 Alloy. In: *Green Materials and Advanced Manufacturing Technology.* Boca Raton: CRC Press; 2020. p.161–172.
13. Sameh SH. Study of the parameters in electrical discharge machining through response surface methodology approach. *Applied Mathematical Modelling.* 2009;33(12): 4397–4407.
14. Soveja A, Cicala E, Grevey D, Jouvard J-M. Optimisation of ta6v alloy surface laser texturing using an experimental design approach. *Optics and Lasers in Engineering.* 2008;46(9): 671–678.
15. Natarajan M, Pasupuleti T, Kiruthika J, Kumar V, Duraisamy P, Polanki V. Optimization of Spark Erosion Machining of Monel 400 Alloy for Automobile Applications. In: *International Conference on Advances in Design, Materials, Manufacturing and Surface Engineering for Mobility.* SAE International; 2023. p.2023–20–0140.
16. Pasupuleti T, Natarajan M, Kumar V, Katta LN, Kiruthika J, Silambarasan R. Predictive Modelling and Process Parameter Prediction for Monel 400 Wire Electrical Discharge Machining for Rocket Frames. In: *International Conference on Advances in Design, Materials, Manufacturing and Surface Engineering for Mobility*. SAE International; 2023. p.2023–28–0088.
17. Kulshrestha AS, Haldar B, Unune DR, Dargar AK. Evaluating the Performance of Electrical Discharge Face Grinding on Super Alloy Monel 400. *Materials Research Express.* 2023;10(9): 096516.
18. Narkhede AR. Mathematical Analysis for Optimizing Electro Discharge Machining Parameters and Enhancing Hastelloy Machining Efficiency. *Communications on Applied Nonlinear Analysis.* 2024;31(1s): 106–120.
19. Rajamani D, Kumar MS, Balasubramanian E. Multi-response optimization of plasma arc cutting on Monel 400 alloy through. whale optimization algorithm. In: *Handbook of Whale Optimization Algorithm. Variants, Hybrids, Improvements, and Applications.* 2024. p.373–386.

20. Gupta PK, Gupta MK. Hybrid optimization approach on electrical discharge machining process for hybrid Al-Al2O3/B4C composites. *Materials Physics and Mechanics.* 2022;50(2): 200–215.
21. Shanmughasundaram P. Influence of abrasive water jet machining parameters on the surface roughness of eutectic Al-Si alloy-Graphite composites. *Materials Physics and Mechanics.* 2014;19(1): 1–8.
22. Amuthakkannan P, ArunPrasath K, Manikandan V, Uthayakumar M, Sureshkumar S. Investigation of the machining performance of basalt fiber composites by abrasive water jet machining. *Materials Physics and Mechanics.* 2021;47(6): 830–842.
23. Sivasankar S, Jeyapaul R, Prasad VV. Performance study of various tool materials for electrical discharge machining of hot pressed zrb2. *Multidiscipline Modeling in Materials and Structures.* 2012;8(4): 505–523.
24. Assarzadeh S, Ghoreishi M. A dual response surface-desirability approach to process modeling and optimization of Al2O3 powder-mixed electrical discharge machining (PMEDM) parameters. International *Journal of Advanced Manufacturing Technology.* 2012;64(9–12):1459–1477.
25. Yadav HNS, Das M. Evaluation of plasma parameters' impact on MRR and surface roughness in plasma polishing of fused silica: An investigation of surface characterization. *Vacuum.* 2024;225: 113263.
26. Panda MR, Biswal SK, Sharma YK. Experimental analysis on the effect of process parameters during CNC turning on nylon-6/6 using tungsten carbide tool. *International Journal of Engineering Sciences & Research Technology.* 2016;5(4): 79–84.
27. Arun Kumar NE, Ganesh M, Vivekanandan N. Optimization of machining parameters in WEDM of Monel 400 using Taguchi technique. *Materials Today: Proceedings.* 2020;22: 2199–2206.
28. Mohanty A, Gangadharudu T, Gangopadhyay S. Experimental investigation and analysis of EDM characteristics of Inconel 825. *Materials and Manufacturing Processes.* 2014;29(5): 540–549.
29. Hourmand M, Farahany S, Sarhan AAD, Yusof NM. Investigating the electrical discharge machining (EDM) parameter effects on Al-Mg2Si metal matrix composite (MMC) for high material removal rate (MRR) and less EWR–RSM approach. *The International Journal of Advanced Manufacturing Technology.* 2015;77(5): 831–838.
30. Naik S, Das SR, Dhupal D. Analysis, predictive modelling and multi-response optimization in electrical discharge machining of Al-22 %SiC metal matrix composite for minimization of surface roughness and hole overcut. *Manufacturing Review.* 2020;7: 20.